HHS Public Access

Author manuscript

Dev Cell. Author manuscript; available in PMC 2021 August 24.

Published in final edited form as:

Dev Cell. 2020 August 24; 54(4): 447–454.e4. doi:10.1016/j.devcel.2020.06.019.

Dietary Lipids Induce Ferroptosis in *Caenorhabditis elegans* and Human Cancer Cells

Marcos A. Perez[1], **Leslie Magtanong**[2], **Scott J. Dixon**[2], **Jennifer L. Watts**[1,*]

[1]School of Molecular Biosciences and Center for Reproductive Biology, Washington State University, Pullman, WA, USA

[2]Department of Biology, Stanford University, Stanford, CA, USA

SUMMARY

Dietary lipids impact development, homeostasis, and disease, but links between specific dietary fats and cell fates are poorly understood. Ferroptosis is an iron-dependent form of nonapoptotic cell death associated with oxidized polyunsaturated phospholipids. Here, we show that dietary ingestion of the polyunsaturated fatty acid (PUFA) dihomogamma-linolenic acid (DGLA; 20:3n-6) can trigger germ cell ferroptosis and sterility in the nematode *Caenorhabditis elegans.* Exogenous DGLA is also sufficient to induce ferroptosis in human cells, pinpointing this omega-6 PUFA as a conserved metabolic instigator of this lethal process. In both *C. elegans* and human cancer cells, ether lipid synthesis protects against ferroptosis. These results establish *C. elegans* as a powerful animal model to study the induction and modulation of ferroptosis by dietary fats and indicate that endogenous ether lipids act to prevent this nonapoptotic cell fate.

ETOC

Ferroptosis is a form of regulated cell death associated with oxidized lipids. Perez et al. report that ingestion of polyunsaturated fatty acids can trigger ferroptosis in *C. elegans* germ cells and human cancer cells. In both systems, endogenous ether lipids protect cells from ferroptotic cell death.

Graphical Abstract

[*]Lead contact: jwatts@wsu.edu.

AUTHOR CONTRIBUTIONS

Conceptualization: J.L.W. and S.J.D. Methodology and Investigation: M.A.P., L.M.; Writing, editing, and reviewing: M.A.P., L.M., S.J.D., J.L.W.; Funding acquisition and Supervision: J.L.W. and S.J.D.

DECALRATION OF INTERESTS

S.J.D. is a member of the scientific advisory board of Ferro Therapeutics.

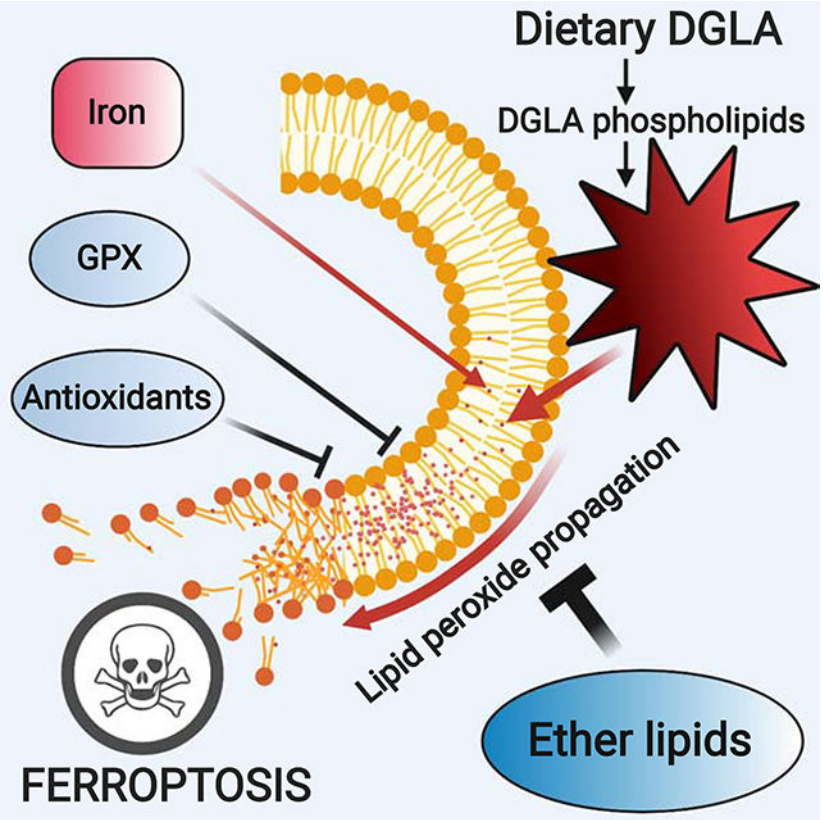

INTRODUCTION

Long-chain polyunsaturated fatty acids (PUFAs), classified as omega-6 (n-6) or omega-3 (n-3), depending on the position of the terminal double bond in the molecule, are essential in the human diet (Saini and Keum, 2018). Omega-6 fatty acids are precursors for powerful proinflammatory signaling molecules that are important for fighting pathogens as well as for normal reproduction, but excess omega-6 fatty acids are associated with disease states, such as cardiovascular disease and cancer (Harris et al., 2009). How different PUFA species influence specific phenotypes at the cellular level remains poorly understood.

Ferroptosis, an iron-dependent form of non-apoptotic cell death, is defined by three conserved hallmarks - the presence of oxidized PUFAs, redox-active iron, and compromised lipid peroxide repair (Dixon and Stockwell, 2019). Ferroptosis has been demonstrated in several mammalian systems, including various cancer cell lines and mice lacking the glutathione-dependent phospholipid hydroperoxidase *Gpx4* (Ingold et al., 2018). In mammalian systems, ferroptosis is suppressed by small molecule iron chelators and radical trapping antioxidants (Stockwell et al., 2017). In vitro, modulating the levels of various metabolites, including monounsaturated fatty acids (MUFAs), can have profound effects on ferroptosis sensitivity (Magtanong et al., 2019); Stockwell et al., 2017). How diet may impact ferroptosis in vivo is less clear. Progress here has been hindered by the absence of accessible and easy-to-manipulate animal models of ferroptosis.

Previously, we discovered that *C. elegans* cultured in the presence of dihomogamma-linolenic acid (DGLA, 20:3n-6) became sterile due to the loss of germ cells, sperm, and oocytes (Watts and Browse, 2006). Genetic pathways regulating oxidative stress responses, lipid homeostasis, and lifespan modulated the sensitivity to dietary DGLA (Watts and Browse, 2006; Webster et al., 2013), as did the manipulation of PUFA oxidation enzymes (Deline et al., 2015). These studies led us to test the hypothesis that dietary DGLA-induced germ cell death occurs via ferroptosis. Here, we report that iron, reactive oxygen species (ROS) and lipid metabolism modulate the effects of dietary DGLA on the worm reproductive system. Furthermore, DGLA supplementation is sufficient to induce ferroptosis in human cancer cells. Finally, endogenous ether lipids play a protective role in protecting both nematode and human cells from ferroptotic cell death, highlighting the conserved nature of this nonapoptotic mechanism.

RESULTS

Dietary DGLA triggers ferroptotic germ cell death

Dietary DGLA is a potent inducer of germ cell death in *C. elegans* (Deline et al., 2015; Watts and Browse, 2006; Webster et al., 2013). To test if DGLA can induce ferroptosis, we co-treated wild-type animals with this PUFA and the ferroptosis-specific radical trapping antioxidant inhibitor ferrostatin-1 (Fer-1) (Dixon et al., 2012; Zilka et al., 2017). Strikingly, in animals co-treated with DGLA and Fer-1, both germ cell death and sterility were reduced compared to worms treated with DGLA alone (Figure 1A). When visualized with DAPI, the number of worms with normal gonad size and morphology were increased in the worm treated with both DGLA and Fer-1 compared to those treated with DGLA alone (Figures 1B,C). Fer-1 by itself had no effect on worm fertility.

DGLA-induced germ cell death is accompanied by an increase of apoptotic corpses, however, DGLA can still induce cell death and sterility in apoptosis-defective *ced-3* and *ced-4* mutants (Watts and Browse, 2006; Webster et al., 2013). Thus, we investigated whether a Fer-1-sensitive mechanism could contribute to germ cell death in parallel to apoptosis. Consistent with this notion, Fer-1 fully suppressed the sterility of *ced-3* mutants exposed to DGLA, indicating that ferroptosis and apoptosis are both activated in response to dietary DGLA (Figure 1A). The lipophilic antioxidant vitamin E derivative Trolox also suppressed sterility in DGLA-treated worms, consistent with the notion that lipid ROS formation was required for DGLA-induced germ cell death (Figures 1D,E). Together, these results suggested that dietary DGLA induces ferroptosis in *C. elegans* germ cells.

DGLA-induced sterility is modulated by redox and iron metabolism

To further explore the hypothesis that dietary DGLA could trigger ferroptosis in *C. elegans* germ cells, we examined additional conserved regulatory nodes. In mammalian cells, GPX4 is a potent inhibitor of ferroptosis, while this process can be promoted by the ROS-producing enzyme NADPH oxidase (NOX)(Dixon et al., 2012; Xie et al., 2017; Yang et al., 2014). We treated *gpx-1* mutants (Sakamoto et al., 2014) with DGLA and found that they are more susceptible to sterility induced by dietary DGLA (Figure 1F). Moreover, a loss of function mutation in *bli-3,* the sole *C. elegans* NOX homolog (Chávez et al., 2009), rendered

the worms resistant to DGLA (Figure 1G). Thus, as in mammals (Ingold et al., 2018), phospholipid glutathione peroxidases protect *C. elegans* germ cells from ferroptosis induced by dietary fatty acids, while NOX-generated ROS contributes to the cell death instigated by dietary DGLA.

Another key a hallmark of ferroptosis is the accumulation of redox-active iron (Stockwell et al., 2017). Intracellular iron is bound to ferritin, encoded in *C. elegans* by the *ftn-1* gene. Ferritin controls iron release in a non-toxic manner, and consequently, *ftn-1* mutants have elevated levels of intracellular iron (Valentini et al., 2012). We observed that *ftn-1* mutants were more susceptible to dietary DGLA-induced cell death than wild-type animals (Figure 1H). Furthermore, treating both wild-type and *ftn-1* worms with the intracellular iron chelator 2,2'-bipyridine suppressed the sterility induced by dietary DGLA (Figure 1H). Thus, DGLA-induced germ cell death in *C. elegans* is modulated by redox and iron metabolism, much like ferroptosis in mammalian cells.

Dietary and endogenous MUFAs inhibit germ cell ferroptosis

In mammalian cells, the addition of exogenous MUFAs such as oleic acid (OA) protect cells from ferroptosis by reducing PUFA incorporation into cellular membranes and dampening lipid ROS accumulation (Magtanong et al., 2019). To test whether exogenous OA could protect *C. elegans* germ cells from dietary DGLA-induced sterility in an analogous manner, we fed wild-type worms various combinations of OA and DGLA. Similar to mammalian cells, we observed strong reduction of DGLA-induced sterility when OA was included in the culture medium (Figure 1I). Gas chromatography-mass spectrometry (GC-MS) analysis of whole-worm fatty acid composition indicated that dietary OA was incorporated into worm lipids, increasing the relative levels of OA compared to vehicle-treated worms. Levels of 18:2n-6 (LA) and 20:5n-3 (EPA) also increased, but relative levels of other C20 PUFAs, including DGLA and AA, were lowered in conjunction with OA supplementation (Table S2). This is consistent with the notion that dietary OA protects cells from ferroptosis by displacing DGLA and AA from cellular membranes.

To further bolster the model that incorporation of DGLA into membrane phospholipids promoted ferroptosis in *C. elegans,* we sought to perturb this process using a genetic approach. The *fat-2* gene encodes a delta-12 fatty acid desaturase, and *fat-2* mutants are unable to convert OA to LA. Consequently, they accumulate high levels of OA in all lipids and lack C18 and C20 PUFAs (Watts and Browse, 2002). Based on our results with exogenous OA, we hypothesized that the accumulation of endogenous OA in *fat-2* mutants would protect from DGLA-induced sterility. Note that approximately 25% of *fat-2* worms are sterile in the absence of dietary DGLA due to lack of PUFAs required for efficient reproduction (Figure 1J). This basal sterility was rescued by dietary DGLA, and furthermore, the *fat-2* worms were almost completely protected from DGLA-induced germ cell death, even though the worms accumulated DGLA to levels that normally cause sterility in wild-type worms. This protection was associated with high levels OA in the corresponding worm lipids (Table S2). Thus, elevating MUFA levels with either genetic or dietary manipulation is sufficient to prevent DGLA-induced germ cell death.

DGLA induces ferroptosis in human cancer cells

In mammalian cells, ferroptosis is typically induced by blocking cystine uptake (e.g. using the small molecule system x_c^- inhibitor, erastin) or directly inhibiting GPX4, and this lethal process can be enhanced by the addition of exogenous PUFAs including arachidonic acid and others (Viswanathan et al., 2017; Zou et al., 2020). Whether exogenous PUFAs are sufficient to induce ferroptosis alone is, however, unclear. To investigate whether exogenous DGLA alone could induce ferroptosis we treated ferroptosis-sensitive HT-1080 fibrosarcoma cells with DGLA (500 μM) and monitored cell death. The cells employed here stably expressed the live cell marker nuclear-localized mKate2 (denoted HT-1080^N) and were incubated in medium containing the dead cell marker SYTOX Green, enabling us to quantify cell death accurately using the scalable analysis of cell death kinetics method (Forcina et al., 2017). Like the positive control erastin2, DGLA triggered cell death in HT-1080 cells that was completely blocked by co-treatment with Fer-1 (Figure 2A,B). DGLA also caused Fer-1-sensitive cell death in HEK-293^N cells, indicating that the ability of exogenous DGLA to induce ferroptosis was not cell-type restricted (Figure 2C). Mechanistically, DGLA caused a significant accumulation of lipid ROS on multiple internal membranes, as detected using the lipid ROS probe C11 BODIPY 581/591 (Pap et al., 1999), and this was prevented by co-incubation with Fer-1 (Figure 2D). Collectively, these results suggested that DGLA treatment alone was capable of inducing ferroptosis in human cells. Of note, other exogenous PUFAs, including arachidonic acid (C20:4n-6), eicosapentaenoic acid (C20:5n-3), and docosahexaenoic acid (C22:6n-3), did not trigger ferrostatin-1-sensitive ferroptosis alone (Figure 2E,F). Thus, the pro-ferroptotic effects of DGLA appear relatively unique.

We further explored the nature of DGLA-induced cell death in human HT-1080 cells. The kinetics of DGLA-induced death were slow compared to erastin2, possibly due to the need to take up and incorporate this fatty acid into cellular phospholipids. Compared to 500 μM treatment, a lower dose of DGLA (e.g. 250 μM) was not lethal to HT-1080^N cells (Figure 2G), indicating that a relatively high dose of this lipid was necessary to overcome the endogenous defense mechanisms of the cell and induce ferroptosis. We examined DGLA uptake and incorporation in phospholipids and neutral lipids using thin-layer chromatography (TLC) and GC-MS. HT-1080^n cells treated with a lethal concentration of DGLA (500 μM, 6 h) exhibited a substantial increase in C20:3-containing phosphatidylcholines (PCs) and triacylglycerols (neutral lipids), with less accumulation in phosphatidylethanolamines (PEs) (Figure 2H, Table S2). Slightly higher C20:3 incorporation into PCs, but not PEs, was observed at a lethal (500 μM) versus non-lethal (250 μM) DGLA concentration (Figure 2H). We also observed decreased acylation of PCs and PEs with MUFA acyl chains (e.g. 18:1n-9) at both lethal and non-lethal concentrations (Figure 2H), indicating that an increase in PUFA-containing phospholipids and the simultaneous loss of protective MUFA-containing phospholipids could both contribute to the induction of ferroptosis in human cells. These results indicate that DGLA is sufficient to induce ferroptosis, possibly via direct modulation of membrane phospholipid acylation.

Ether lipid deficiency exacerbates DGLA-induced ferroptosis

The functions of ether-linked lipids in cells is relatively understudied. We previously found that *C. elegans* strains that are defective in ether lipid biosynthesis are sensitive to oxidative stress induced by tert-butyl peroxide or paraquat (Shi et al., 2016). The *C. elegans ads-1* gene encodes alkylglycerone phosphate synthase (AGPS), which catalyzes the rate-limiting step for ether lipid biosynthesis. Compared to wild-type controls, ether-lipid deficient *ads-1* mutants were hypersensitive to DGLA-induced sterility (Figure 3A). Importantly, whole worm lipidomic analysis revealed that *ads-1* mutants lack plasmalogens and the uptake of DGLA was similar or slightly lower than in the wild-type controls (Table S2). The *ads-1* mutants grown on lower doses of DGLA caused considerable sterility that was reduced by the addition of Fer-1 (Figure 3A). Therefore, endogenous ether lipid synthesis strongly protects *C. elegans* from dietary DGLA-induced ferroptosis.

Previous studies indicate that ether lipids may act as endogenous antioxidant molecules (Engelmann, 2004; Shi et al., 2016; Wallner and Schmitz, 2011). We investigated whether this property might contribute to protection from ferroptosis in DGLA-treated worms. In support of this model, the iron chelator 2,2’ bipyridine potently suppressed DGLA-induced ferroptosis in both wild-type and DGLA-hypersensitive *ads-1* mutants (Figure 3B). Moreover, the addition of dietary OA was able to partially suppress the germ cell death in the *ads-1* strain (Figure 3C). By contrast, disruption of *bli-3* did not reduce the sensitivity of *ads-1* mutants to DGLA (Figure 3D). Thus, even in the absence of sensitizing NOX activity, ether lipids appear required to protect against DGLA-induced ferroptosis. Finally, we previously showed that removing endogenous synthesized PUFAs using the *fat-3* mutant, which accumulates C18:2 and C18:3, but depletes all C20 PUFAs, leads to resistance against dietary DGLA (Watts and Browse, 2006). Strikingly, the *ads-1;fat-3* double mutants show resistance at the same levels as *fat-3* mutants alone (Figure 3D). This suggests that endogenously synthesized ether lipids protect cells from ferroptosis by inhibiting the propagation of lipid peroxides in PUFA-rich membranes.

Given these results, we examined whether ether lipids could modulate ferroptosis in human cells. ZINC-69435460 (herein referred to as “AGPSi”) is a specific inhibitor of mammalian AGPS (Piano et al., 2015). Consistent with results obtained in worms, pretreatment for 24 h with AGPSi sensitized HT-1080^{N} cells to cell death induced by DGLA, as well as the ferroptosis-inducing GPX4 inhibitor RSL3 (Figure 3E). This sensitization effect was specific, as AGPSi pretreatment had no effect on the lethality of bortezomib, a proteasome inhibitor that induces apoptosis (Figure 3E). Co-treatment with Fer-1 suppressed cell death completely in response to RSL3, and partially in response to DGLA (Figure 3E), akin to the partial suppression of cell death by Fer-1 in *ads-1* mutant DGLA-treated worms (Figure 3A). Thus, a protective role for ether lipid synthesis against ferroptosis appears to be conserved between species.

DISCUSSION

Here we report that ferroptosis can be induced in *C. elegans* germ cells and mammalian cells exposed to DGLA. The germ cell death shares many characteristics of ferroptosis in mammalian cells (Table 1 and references therein). The specificity of DGLA-induced

ferroptosis for the germ cells of young animals is of great interest. Dietary lipids may be preferentially concentrated in these cells during the rapid and metabolically demanding process of cell formation that occurs in the syncytial gonad. Another possibility is that the germline itself may be deficient in antioxidant defenses (or enriched in prooxidant enzymes) that render these cells hypersensitive to the accumulation of lipid peroxides compared to somatic cells. Interestingly, ferroptosis may also occur in intestinal cells of aged *C. elegans* (Jenkins et al., 2019). Here, the aging process itself may lead to the loss of control over iron homeostasis or other processes that normally restrain ferroptosis in somatic tissues. Together, these results establish *C. elegans* as a powerful and genetically tractable animal model of ferroptosis.

Germ cell death can be induced in *C. elegans* by dietary DGLA, and to a lesser extent dietary AA. We do not observed cell death induced by dietary linoleic acid (LA), or omega-3 PUFAs such as linolenic acid (ALA), 20:3n-3 or EPA (Watts and Browse, 2006). We speculate that the ability of DGLA to specifically induce ferroptosis in *C. elegans* germ cells, as well as in human cells as single agents, could be explained by selective structure-specific peroxidation by CYP or LOX enzymes (Deline et al., 2015; Kagan et al., 2017; Yang et al., 2016; Zou et al., 2020). This lipid peroxide will then auto-catalyze the formation of other lipid peroxides on neighboring PUFAs, ultimately leading to membrane permeabilization (Figure 3G). One possibility suggested by this work is that combining exogenous DGLA with small molecule inducers of ferroptosis may represent an especially effective means of inducing ferroptosis in cancer cells, as well as in other sensitive cell types in vivo.

Endogenous ether lipids may oppose lipid ROS propagation by acting as oxidative ‘sinks’ to protect nearby PUFA acyl chains from oxidation (Engelmann, 2004; Shi et al., 2016; Wallner and Schmitz, 2011). It is notable that in mammalian cells ether lipids are concentrated on the cytosolic leaflet of the plasma membrane where potentially oxidizable PUFA species are more abundant, and the need for counterbalancing antioxidant activity therefore presumably highest (Lorent et al., 2020). Humans born with defective ether lipid synthesis enzymes have severe growth and mental deficiencies and most do not survive beyond childhood (Wanders and Waterham, 2006). Our findings raise the possibility that the failure to combat lipid propagation and cellular oxidative stress, and perhaps the failure to prevent excessive ferroptotic cell death after exposure to dietary PUFAs, may contribute to the observed developmental defects.

STAR METHODS

RESOURCE AVAILABILITY

Lead Contact—Further information and requests for resources and reagents should be directed to and will be fulfilled by the Lead Contact, Jennifer Watts (jwatts@wsu.edu).

Materials Availability—*C. elegans* strains generated for these studies are available upon request.

Data and Code Availability—The published article includes all datasets [generated or analyzed during this study.

EXPERIMENTAL MODEL AND SUBJECT DETAILS

***C. elegans* strains and maintenance—**Nematode stocks were maintained on nematode growth media (NGM) plates seeded with bacteria *(E. coli* OP50) at 20°C. The following strains/alleles used in this study were obtained from the *Caenorhabditis* Genetics Center (CGC): N2 Bristol (wild-type), MT1522 *ced-3(n717),* CB767 *bli-3(e767).* The GA912 *ftn-1(ok3625)* strain was a gift from Dr. David Gems (University College London, London, UK). The *gpx-1(tm2100)* strain was obtained from the National Bio-Resource Project (Tokyo, Japan) and outcrossed 3x against N2. The *ads-1(wa3), fat-2(wa17),* and *fat-3(wa22)* strains were created in the Watts laboratory (Shi et al., 2016; Watts and Browse, 2002).

Cell lines and chemicals—HT-1080 cells (Cat# ATCC CCL-121; gender: male) were purchased from ATCC, expanded for one passage, aliquoted and frozen down at −140°C until use. HT-1080^{N} cells were described previously (Forcina et al., 2017). HEK 293^{N} cells were derived from the parental cell line described previously (Magtanong et al., 2019). Polyclonal populations of this cell line were transduced with lentivirus directing the expression of nuclear-localized mKate2 (Cat# 4476, Essen BioSciences, Ann Arbor, Michigan, USA), as described previously (Forcina et al, 2017). Erastin2 (compound 35MEW28 in (Dixon et al., 2014)) was synthesized by Acme Bioscience (Palo Alto, CA). 1*S*,3*R*-RSL3 (RSL3, Cat# S8155) was from Selleck Chemicals (Houston, TX). Dimethyl sulfoxide (DMSO, Cat# 276855) and ferrostatin-1 (Cat# SML0583) were from Sigma-Aldrich (St. Louis, MO). Ethanol (Cat# AX0441–3) was from EMD Millipore (Billerica, MA). Dihomo-γ-linolenic acid (DGLA, Cat# 90230), arachidonic acid (Cat# 90010), docosahexaenoic acid (Cat# 90310) and eicosapentaenoic acid (Cat# 90110) were from Cayman Chemical (Ann Arbor, MI). SYTOX Green (Cat# S7020) was from Molecular Probes (Eugene, OR). All compounds were stored at −20°C.

HEK-293^{n} cells were grown in Dulbecco's modified Eagle medium (DMEM, Cat# MT-10–013-CV, Thermo Fisher Scientific, Waltham, MA), 10% fetal bovine serum (FBS, Cat# 26140079, Gibco) and 0.5 U/mL Pen/Strep (P/S, Cat# 15070–063, Gibco). HT-1080 cells were grown in DMEM supplemented with 10% FBS, 0.5 U/mL P/S and 1x non-essential amino acids (NEAAs, Cat# 11140–050, Gibco). Hanks' Balanced Salt solution (HBSS, Cat# 14025–134) and trypsin (Cat# 25200114) were from Gibco. For all experiments, cells were trypsinized and counted using a Cellometer Auto T4 cell counter (Nexcelom, Lawrence, MA, USA).

METHODS DETAILS

Construction of double mutant strains—The *bli-3(e767);ads-1(wa3)* double mutant strain was constructed by crossing *ads-1* males to *bli-3* hermaphrodites. F1 cross progeny were allowed to self and F2 progeny with blisters were grown individually on NGM plates. When the F3 progeny from individual F2 matured and reproduced, and the bacterial lawn was depleted, the F3+F4 generations were harvested in bulk from each plate and the population was analyzed by GC/MS. Strains lacking plasmalogen were identified as

homozygous *ads-1* mutants. The BX291 *ads-1(wa3);fat-3(wa22)* double mutant strain was constructed by crossing *ads-1* males with *fat-3* hermaphrodites, allowing the F1 cross progeny to self and plating F2 progeny individually. After the F3 matured and reproduced, the plates were harvested as described above, and analyzed with GC/MS for the combined absence of C20 PUFAs and plasmalogens.

Fatty acid supplementation for *C. elegans* sterility assay—The fatty acid supplemented media was previously described (Deline et al., 2013). To NGM media, 0.1% Tergitol NP40 (Sigma Chemicals Cat#NP40S) and the sodium salt of dihomo-gamma-linolenic acid (DGLA, 20:3n-6) (NuChek Prep, Inc. Cat#S-1143) or oleic acid (OA, 18:1 n-9) (NuChek Prep, Inc. Cat#S-1120) were added at various concentrations ranging from 0.1mM to 0.3mM DGLA. *E. coli* OP50 food source were seeded plates 3 days prior to plating *C. elegans* L1 synchronized larvae. Adult worms were scored for sterility at 72–96 hours where sterility was determined by scoring worms with absences of embryos as indicated by an empty uterus with light microscopy. The sterility tests were scored and averaged over five individual plates of each genotype, each consisting of 50 nematodes. Sterility was compared between control populations and experimental populations using a two-tailed student's t-test. Exogenous fatty acid uptake of nematodes was confirmed through direct transesterification of nematode populations using 2.5% H_2SO_4 for one hour at 70°C to generate fatty acid methyl ester (FAMEs). FAMES were extracted with hexane for gas chromatography/mass spectrometry (GC/MS) analysis (Watts and Browse, 2002). Uptake analysis determined that the presence of DMSO increases DGLA uptake in worms, while certain *E. coli* strains, such as HT115, used for RNAi feeding, require the use of higher concentrations of DGLA than E. coli OP50.

Ferrostatin-1 and DGLA supplementation—DGLA plates were made ahead of time by adding various concentrations to molten NGM agar prior to plating. OP50 was plated and allowed to dry for two days prior to plating drugs and worms. The ferrostatin-1 (Fer-1) (Sigma-Aldrich Cat#SML0583) was dissolved in dimethyl sulfoxide (DMSO, Cat# 276855) and diluted to the appropriate concentrations in 10% DMSO prior to plating onto the OP50 food source shortly. The Fer-1 solution or control DMSO was allowed to absorb into the plates for 20–30 minutes before adding L1 stage nematodes.

Trolox and 2,2'-bipyridine (BP) DGLA supplementation—2,2-bipyridiyl (BP) (Sigma-Aldrich Cat# D216305) (75pm) or Trolox (Cayman Chemicals Cat#10011659) were added directly to NGM agar. Either the drug or the equivalent volume amount of vehicle, DMSO, were added to molten along with various concentrations of DGLA into NGM agar prior to pouring into plates.

DAPI staining for germ cell visualization—To visualize germ cells after feeding (either DGLA / DMSO, DGLA / 250μM Fer-1, or DGLA/1mM Trolox) worms were washed off with 1mL of M9 buffer and dispensed onto a watch glass. The majority of the M9 buffer was blotted dry, and worms were then fixed and stained with ethanol containing 0.2μg/mL 2',6-diamidino-2-phenylindole (DAPI) (Fisher Scientific, Cat#D1306) and allowed to fix and stain for 10 minutes. Worms were placed on a coverslip with a droplet of water and

adhered to a 2% agar pad containing slide. Images were acquired using an Olympus BX53 microscope (Olympus, Shinjuku, Tokyo, Japan) with a 10X objective lens.

Cell death experiments—For co-treatment experiments, the day before the experiment, 5,000 HT-1080^{N} or 20,000 HEK-293^{n} cells/well were seeded into a 96-well plate (Cat# 3904, Corning). The next day, the cell culture medium was replaced with the appropriate compound treatments. For pre-treatment experiments, the day before the pre-treatment, 2,000 HT-1080^{N} cells/well were seeded into a 96-well plate. The next day, the cell culture medium was replaced with medium containing DMSO (vehicle) or ZINC-69435460 (500 μM). 24 h later, the medium was replaced with the appropriate compound treatments. For all experiments, SYTOX Green (20 nM) was included. Cells were imaged on the Essen IncuCyte Zoom (Ann Arbor, MI) and analyzed as described (Forcina et al., 2017). At least three independent biological experiments were performed for each condition.

C11 581/591 BODIPY imaging—The day before the experiment, 125,000 HT-1080 cells/well were seeded into 6-well plates (Cat# 3516, Corning) with one 22 mm^2 no. 1.5 glass coverslip in each well. The next day, the cells were treated with vehicle (ethanol) or DGLA (500 μM) and DMSO or ferrostatin-1 (1 μM) in HT-1080 growth medium at 37°C for 8 h. After 8 h, the medium was removed and the cells were treated with C11 BODIPY 581/591 (Cat# D3861, Molecular Probes, Eugene, OR; final concentration = 5 μM) and Hoechst (Cat# H1399, Molecular Probes; final concentration = 1 μg/mL) dissolved in HBSS and incubated at 37°C for 10 min. After 10 min, the C11 BODIPY 581/591/Hoechst mixture was removed and fresh HBSS was added to the cells. Each cover slip was removed and mounted in 25 μL HBSS onto a glass microscope slide. Cells were imaged using a Zeiss Axio Observer microscope with a confocal spinning-disk head (Yokogawa, Tokyo, Japan), PlanApoChromat 63*/1.4 NA oil immersion objective, and a Cascade II:512 electron-multiplying (EM) CCD camera (Photometrics, Tucson, AZ). Images were processed in ImageJ 1.48v. Imaging was performed on two independent biological replicates per treatment condition.

Mammalian cell lipid analysis—For DGLA-treated cells, the day before the experiment, 2×10^6 HT-1080 cells/plate were seeded into 10 cm dishes (Cat# CC7682–3394, USA Scientific, Ocala, FL). Four 10 cm dishes were seeded for each treatment. The next day, cells were treated with ethanol (vehicle) or dihomo-gamma-linoleic acid (Cat# 90230, Cayman Chemical, 250 μM or 500 μM) for 6 h. For AGPSi-treated cells, the day before the experiment, 750,000 HT-1080^{N} cells/plate were seeded into 10 cm dishes. The next day, cells were treated with DMSO (vehicle) or ZINC-69435460 (Cat# Z1030248250, Enamine, Cincinnati, OH, 500 μM) for 24 h. For both experiments, at the end of treatment time, the media was removed and each plate was washed 1–3 times with 3 mL 1x phosphate buffered saline, pH 7.4 (PBS, Cat# 10010023, Gibco). After the final wash, 2 mL of 1x PBS was added to each plate. Cells were scraped off each plate and transferred via glass Pasteur pipette to a conical bottomed glass tube (Cat# 05–569-2, Fisher Scientific), resulting in ~8 mL total cell suspension per treatment for DGLA-treated cells and 2 mL for AGPSi-treated cells. 0.5 mL was removed for protein determination. Each cell suspension (for both lipidomics and protein determination) was centrifuged (1000 rpm, 5 min, room

temperature), the supernatant was removed using a glass Pasteur pipette, and the cell pellet was immediately stored at −80 °C, prior to further analysis. Protein concentration was determined using a BCA assay kit (Pierce).

For lipid analysis of DGLA-treated cells, the remaining cell pellet was extracted over night at −20°C in 5 mL of ice-cold 5 mL chloroform:methanol (1:1). A solution of 0.2M H_3PO_4, 1M KCl was added to samples, which resulted in phase separation of the organic and aqueous phase. The organic phase was removed and dried under argon, then resuspended in chloroform. Samples were loaded in triplicate with authentic standards and TLC plates were developed in a solvent system consisting of chloroform:methanol:water:acetic acid (65:43:3:2.5). Lipids were visualized under UV light after spraying the plate with 0.005% primuline, and spots corresponding to phosphatidylcholine (PC), phosphatidylethanolamine (PE) and neutral lipids were scraped, spiked with a known standard (15:0), and transesterified in 2.5% H_2SO_4 to generate FAMES for GC/MS analysis to determine the fatty acid composition of each lipid class (Watts and Browse, 2002). Three biological replicates were used for TLC analysis. Direct transesterification and GC/MS analysis was performed with the remaining cell pellet of the AGPSi-treated cells.

QUANTIFICATION AND STATISTICAL ANALYSIS

Lethal fraction scoring was performed using Microsoft Excel 16.16.19 (Microsoft Corporation, Redmond, WA). Graphing and statistical analyses were performed using Prism 8.3.1 (GraphPad Software, La Jolla, CA). Confocal images were processed in ImageJ 1.52q (U.S. National Institutes of Health, Bethesda, MD). Figures were assembled using Photoshop and Adobe Illustrator 24.0 (Adobe Systems, San Jose, CA). Statistical details of experiments and statistical tests used can be found in the main text, figure legends, and supplemental tables.

Supplementary Material

Refer to Web version on PubMed Central for supplementary material.

ACKNOWLEDGEMENTS

Some nematode strains were provided by the Caenorhabditis Genetics Center, funded by NIH Office of Research Infrastructure Programs (P40 OD010440). The GA912 *ftn-1(ok3625)* strain was a gift from Dr. David Gems (University College London, London, UK). The *gpx-1(tm2100)* strain was obtained from the National Bio-Resource Project (Tokyo, Japan). Funding to JLW was provided by the NIH (1R01GM133883), the Farrell Memorial Fund, the Stanly Adler Research fund, and the Donald R. Weldin research fund. Funding to S.J.D. was provided by the NIH (1R01GM122923).

References

Chávez V, Mohri-Shiomi A, and Garsin DA (2009). Ce-Duox1/BLI-3 Generates Reactive Oxygen Species as a Protective Innate Immune Mechanism in *Caenorhabditis elegans*. Infection and Immunity 77, 4983–4989. [PubMed: 19687201]

Deline M, Keller J, Rothe M, Schunck WH, Menzel R, and Watts JL (2015). Epoxides Derived from Dietary Dihomo-Gamma-Linolenic Acid Induce Germ Cell Death in *C. elegans*. Sci Rep 5, 15417. [PubMed: 26486965]

Deline ML, Vrablik TL, and Watts JL (2013). Dietary supplementation of polyunsaturated fatty acids in *Caenorhabditis elegans*. Journal of visualized experiments : JoVE.

Dixon SJ, Lemberg KM, Lamprecht MR, Skouta R, Zaitsev EM, Gleason CE, Patel DN, Bauer AJ, Cantley AM, Yang WS, et al. (2012). Ferroptosis: an iron-dependent form of nonapoptotic cell death. Cell 149, 1060–1072. [PubMed: 22632970]

Dixon SJ, Patel DN, Welsch M, Skouta R, Lee ED, Hayano M, Thomas AG, Gleason CE, Tatonetti NP, Slusher BS, et al. (2014). Pharmacological inhibition of cystine- glutamate exchange induces endoplasmic reticulum stress and ferroptosis. Elife 3, e02523. [PubMed: 24844246]

Dixon SJ, and Stockwell BR (2019). The Hallmarks of Ferroptosis. Annual Review of Cancer Biology 3, 35–54.

Doll S, Proneth B, Tyurina YY, Panzilius E, Kobayashi S, Ingold I, Irmler M, Beckers J, Aichler M, Walch A, et al. (2017). ACSL4 dictates ferroptosis sensitivity by shaping cellular lipid composition. Nat Chem Biol 13, 91–98. [PubMed: 27842070]

Engelmann B (2004). Plasmalogens: targets for oxidants and major lipophilic antioxidants. Biochem Soc Trans 32, 147–150. [PubMed: 14748736]

Fan Z, Wirth AK, Chen D, Wruck CJ, Rauh M, Buchfelder M, and Savaskan N (2017). Nrf2-Keap1 pathway promotes cell proliferation and diminishes ferroptosis. Oncogenesis 6, e371. [PubMed: 28805788]

Forcina GC, Conlon M, Wells A, Cao JY, and Dixon SJ (2017). Systematic Quantification of Population Cell Death Kinetics in Mammalian Cells. Cell systems 4, 600–610 e606. [PubMed: 28601558]

Harris WS, Mozaffarian D, Rimm E, Kris-Etherton P, Rudel LL, Appel LJ, Engler MM, Engler MB, and Sacks F (2009). Omega-6 fatty acids and risk for cardiovascular disease: a science advisory from the American Heart Association Nutrition Subcommittee of the Council on Nutrition, Physical Activity, and Metabolism; Council on Cardiovascular Nursing; and Council on Epidemiology and Prevention. Circulation 119, 902–907. [PubMed: 19171857]

Ingold I, Berndt C, Schmitt S, Doll S, Poschmann G, Buday K, Roveri A, Peng X, Porto Freitas F, Seibt T, et al. (2018). Selenium Utilization by GpX4 Is Required to Prevent Hydroperoxide-Induced Ferroptosis. Cell 172, 409–422 e421. [PubMed: 29290465]

Jenkins NL, James SA, Salim A, Sumardy F, Speed TP, Conrad M, Richardson DR, Bush AI, and McColl G (2019). Ferrous-glutathione coupling mediates ferroptosis and frailty in Caenorhabditis elegans. bioRxiv, 594408.

Kagan VE, Mao G, Qu F, Angeli JP, Doll S, Croix CS, Dar HH, Liu B, Tyurin VA, Ritov VB, et al. (2017). Oxidized arachidonic and adrenic PEs navigate cells to ferroptosis. Nat Chem Biol 13, 81–90. [PubMed: 27842066]

Lorent JH, Levental KR, Ganesan L, Rivera-Longsworth G, Sezgin E, Doktorova M, Lyman E, and Levental I (2020). Plasma membranes are asymmetric in lipid unsaturation, packing and protein shape. Nat Chem Biol.

Magtanong L, Ko PJ, To M, Cao JY, Forcina GC, Tarangelo A, Ward CC, Cho K, Patti GJ, Nomura DK, et al. (2019). Exogenous Monounsaturated Fatty Acids Promote a Ferroptosis-Resistant Cell State. Cell chemical biology 26, 420–432 e429. [PubMed: 30686757]

Matsushita M, Freigang S, Schneider C, Conrad M, Bornkamm GW, and Kopf M (2015). T cell lipid peroxidation induces ferroptosis and prevents immunity to infection. J Exp Med 212, 555–568. [PubMed: 25824823]

Pap EH, Drummen GP, Winter VJ, Kooij TW, Rijken P, Wirtz KW, Op den Kamp JA, Hage WJ, and Post JA (1999). Ratio-fluorescence microscopy of lipid oxidation in living cells using C11-BODIPY(581/591). FEBS Lett 453, 278–282. [PubMed: 10405160]

Piano V, Benjamin DI, Valente S, Nenci S, Marrocco B, Mai A, Aliverti A, Nomura DK, and Mattevi A (2015). Discovery of Inhibitors for the Ether Lipid-Generating Enzyme AGPS as Anti-Cancer Agents. ACS Chem Biol 10, 2589–2597. [PubMed: 26322624]

Saini RK, and Keum YS (2018). Omega-3 and omega-6 polyunsaturated fatty acids: Dietary sources, metabolism, and significance - A review. Life Sci 203, 255–267. [PubMed: 29715470]

Sakamoto T, Maebayashi K, Nakagawa Y, and Imai H (2014). Deletion of the four phospholipid hydroperoxide glutathione peroxidase genes accelerates aging in *Caenorhabditis elegans*. Genes Cells 19, 778–792. [PubMed: 25200408]

Seiler A, Schneider M, Forster H, Roth S, Wirth EK, Culmsee C, Plesnila N, Kremmer E, Radmark O, Wurst W, et al. (2008). Glutathione peroxidase 4 senses and translates oxidative stress into 12/15-lipoxygenase dependent- and AIF-mediated cell death. Cell metabolism 8, 237–248. [PubMed: 18762024]

Shi X, Tarazona P, Brock TJ, Browse J, Feussner I, and Watts JL (2016). A *Caenorhabditis elegans* model for ether lipid biosynthesis and function. J Lipid Res 57, 265–275. [PubMed: 26685325]

Skouta R, Dixon SJ, Wang J, Dunn DE, Orman M, Shimada K, Rosenberg PA, Lo DC, Weinberg JM, Linkermann A, et al. (2014). Ferrostatins inhibit oxidative lipid damage and cell death in diverse disease models. J Am Chem Soc 136, 4551–4556. [PubMed: 24592866]

Stockwell BR, Angeli JPF, Bayir H, Bush AI, Conrad M, Dixon SJ, Fulda S, Gascon S, Hatzios SK, Kagan VE, et al. (2017). Ferroptosis: A Regulated Cell Death Nexus Linking Metabolism, Redox Biology, and Disease. Cell 171, 273–285. [PubMed: 28985560]

Sun X, Ou Z, Chen R, Niu X, Chen D, Kang R, and Tang D (2016). Activation of the p62-Keap1-NRF2 pathway protects against ferroptosis in hepatocellular carcinoma cells. Hepatology 63, 173–184. [PubMed: 26403645]

Valentini S, Cabreiro F, Ackerman D, Alam MM, Kunze MBA, Kay CWM, and Gems D (2012). Manipulation of in vivo iron levels can alter resistance to oxidative stress without affecting ageing in the nematode *C. elegans*. Mech Ageing Dev 133, 282–290. [PubMed: 22445852]

Viswanathan VS, Ryan MJ, Dhruv HD, Gill S, Eichhoff OM, Seashore-Ludlow B, Kaffenberger SD, Eaton JK, Shimada K, Aguirre AJ, et al. (2017). Dependency of a therapy-resistant state of cancer cells on a lipid peroxidase pathway. Nature 547, 453–457. [PubMed: 28678785]

Wallner S, and Schmitz G (2011). Plasmalogens the neglected regulatory and scavenging lipid species. Chem Phys Lipids 164, 573–589. [PubMed: 21723266]

Wanders RJ, and Waterham HR (2006). Peroxisomal disorders: the single peroxisomal enzyme deficiencies. Biochim Biophys Acta 1763, 1707–1720. [PubMed: 17055078]

Watts JL, and Browse J (2002). Genetic dissection of polyunsaturated fatty acid synthesis in *Caenorhabditis elegans*. Proc Natl Acad Sci U S A 99, 5854–5859. [PubMed: 11972048]

Watts JL, and Browse J (2006). Dietary manipulation implicates lipid signaling in the regulation of germ cell maintenance in *C. elegans*. Dev Biol 292, 381–392. [PubMed: 16487504]

Webster CM, Deline ML, and Watts JL (2013). Stress response pathways protect germ cells from omega-6 polyunsaturated fatty acid-mediated toxicity in *Caenorhabditis elegans*. Dev Biol 373, 14–25. [PubMed: 23064027]

Xie Y, Zhu S, Song X, Sun X, Fan Y, Liu J, Zhong M, Yuan H, Zhang L, Billiar TR, et al. (2017). The Tumor Suppressor p53 Limits Ferroptosis by Blocking DPP4 Activity. Cell reports 20, 1692–1704. [PubMed: 28813679]

Yang WS, Kim KJ, Gaschler MM, Patel M, Shchepinov MS, and Stockwell BR (2016). Peroxidation of polyunsaturated fatty acids by lipoxygenases drives ferroptosis. Proc Natl Acad Sci U S A 113, E4966–E4975. [PubMed: 27506793]

Yang WS, SriRamaratnam R, Welsch ME, Shimada K, Skouta R, Viswanathan VS, Cheah JH, Clemons PA, Shamji AF, Clish CB, et al. (2014). Regulation of ferroptotic cancer cell death by GPX4. Cell 156, 317–331. [PubMed: 24439385]

Yang WS, and Stockwell BR (2008). Synthetic lethal screening identifies compounds activating iron-dependent, nonapoptotic cell death in oncogenic-RAS-harboring cancer cells. Chem Biol 15, 234–245. [PubMed: 18355723]

Yang WS, and Stockwell BR (2016). Ferroptosis: Death by Lipid Peroxidation. Trends Cell Biol 26, 165–176. [PubMed: 26653790]

Zilka O, Shah R, Li B, Friedmann Angeli JP, Griesser M, Conrad M, and Pratt DA (2017). On the Mechanism of Cytoprotection by Ferrostatin-1 and Liproxstatin-1 and the Role of Lipid Peroxidation in Ferroptotic Cell Death. ACS Cent Sci 3, 232–243. [PubMed: 28386601]

Zou Y, Li H, Graham ET, Deik AA, Eaton JK, Wang W, Sandoval-Gomez G, Clish CB, Doench JG, and Schreiber SL (2020). Cytochrome P450 oxidoreductase contributes to phospholipid peroxidation in ferroptosis. Nat Chem Biol 16, 302–309. [PubMed: 32080622]

Highlights

- Germ cell death induced by dietary DGLA occurs via ferroptosis in *C. elegans*
- Ferroptotic cell death is alleviated by antioxidants and iron chelators
- DGLA specifically induces ferroptosis in human cancer cells
- Ether lipids protect cells from DGLA-induced ferroptosis

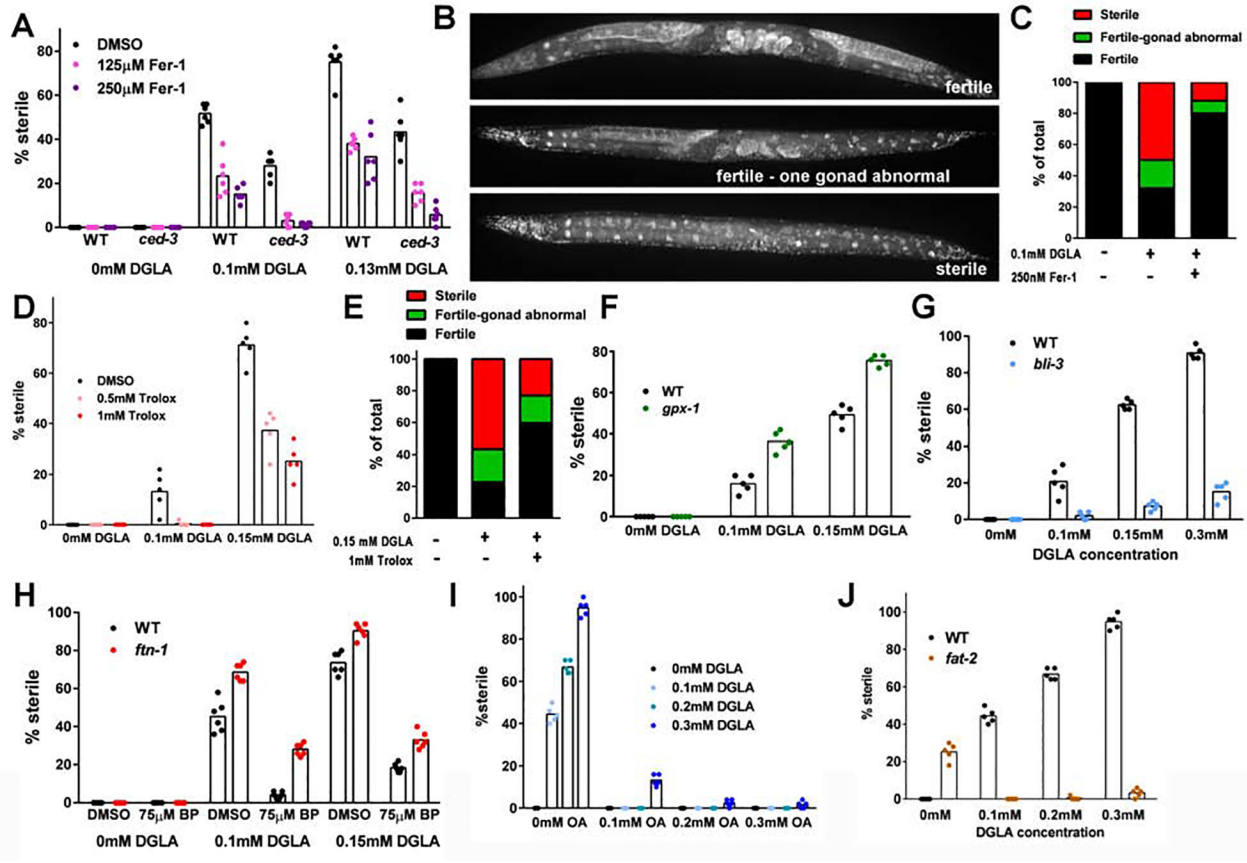

Figure 1. Ferroptosis regulators modulate DGLA-induced germ cell death.

(A) Percentage (%) sterility of wild-type and *ced-3 C. elegans* raised on 0.1 mM or 0.13 mM DGLA and ferrostatin-1 (Fer-1). (B) Representative DAPI-stained images of wild-type *C. elegans* after exposure to 0.1 mM DGLA. Fertile worms may have abnormal (diminished) gonads. (C) Quantification of fertility phenotypes based on the categories in (B). (D) % sterility of worms exposed to DGLA ± Trolox (vitamin E). (E) Quantification of fertility phenotypes based on the categories in (B). (F) % sterility of wild-type or *gpx-1* mutant worms after dietary exposure to DGLA (G) % sterility of wild-type or NADPH oxidase/ duox *(bli-3)* mutant worms after dietary exposure to DGLA. (H) % sterility of wild-type or *ftn-1* mutant worms exposed to dietary DGLA ± 2,2'-bipyridine (BP). (I) % sterility of wild-type worms fed the indicated combinations of oleic acid (OA) and DGLA. (J) % sterility of wild-type and *fat-2* mutants raised on DGLA plates. In (A, D, and F-J), each point represents an independent experiment comprising 50 worms for each treatment. Statistical significance was determined by two-way ANOVA with a Tukey's test for multiple comparisons (Table S1). Fatty acid composition data is reported in Table S2.

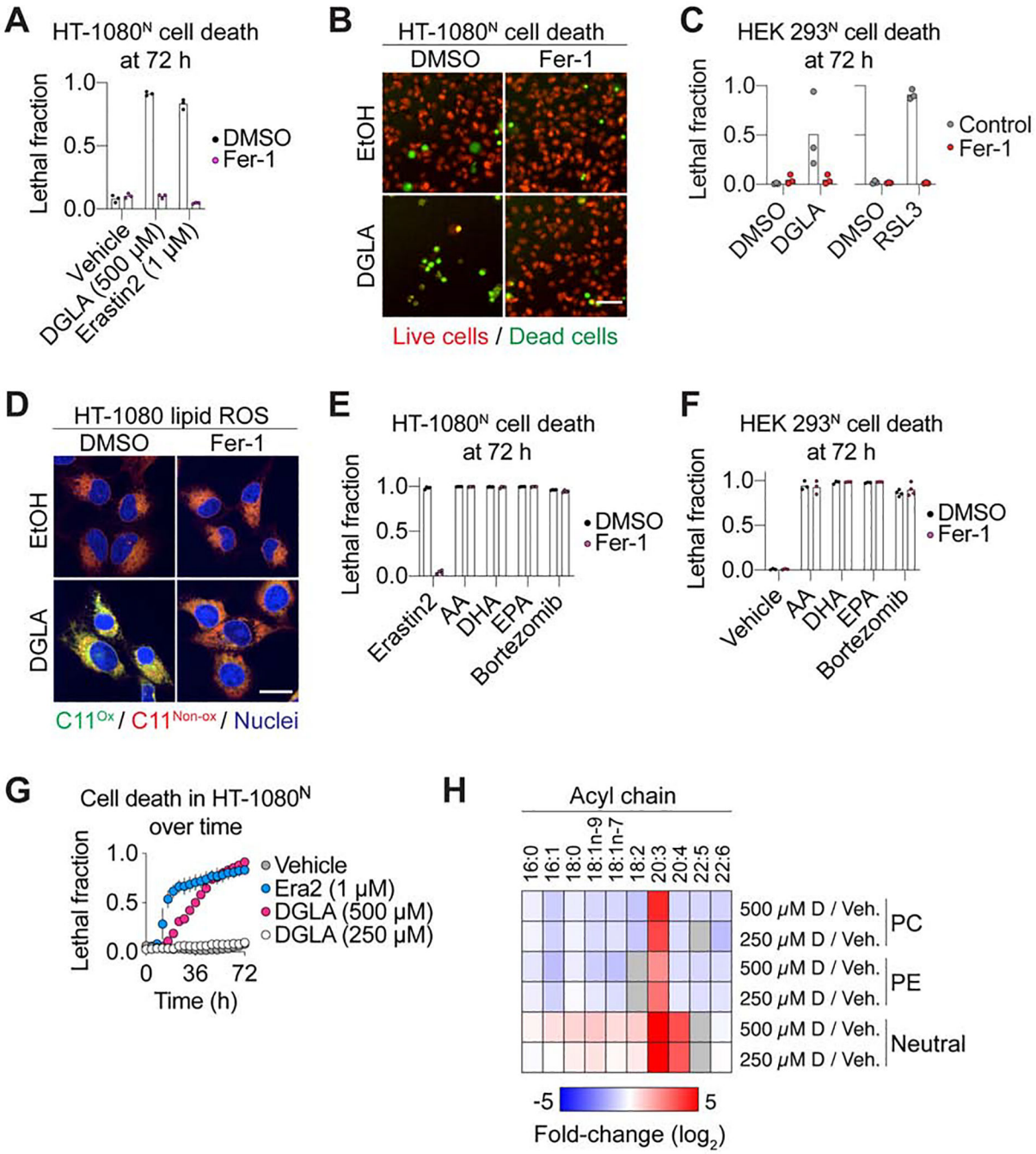

Figure 2. DGLA induces ferroptosis in human cells.

(A) Cell death (lethal fraction) in HT-1080^{n} cells treated ± erastin2, dihomogamma-linolenic acid (DGLA) and ± ferrostatin-1 (Fer-1, 1 μM). (B) Representative images showing HT-1080^{n} cells treated ± DGLA (500 μM) ± Fer-1 (1 μM) at 72 h. Live cells express nuclear-localized mKate2; dead cells take up SYTOX Green. Scale bar = 50 pm. (C) Cell death ± Fer-1 (1 μM). (D) Confocal images of C11 BODIPY 581/591 (herein "C11") in HT-1080 cells. After treatment for 8 h, cells were labeled with C11 (5 μM) and Hoechst (1 μM /mL) prior to imaging. C11^{Ox}: Oxidized C11; C11^{Non-Ox}: Non-Oxidized C11. Scale bar

= 20 μm. Images are representative of two independent experiments. (E,F) Cell death in response to treatment with polyunsaturated fatty acids (all at 500 μM), or a control non-ferroptotic lethal bortezomib (200 nM), ± Fer-1 (1 μM). AA: arachidonic acid, DHA: docosahexaenoic acid, EPA: eicosapentaenoic acid. (G) Cell death over time. (H) Heat map showing the relative fold changes in fatty acid composition of various lipid classes after 6 hours of growth with DGLA (500 μM or 250 μM) versus ethanol controls. PC: phosphatidylcholine, PE: phosphatidylethanolamine, neutral: neutral lipids. Grey boxes indicate situations with fatty acid concentrations at less than 0.4%. Each data point in A,C,E,F represents an independent experiment. Data in G represent mean ± SD of three independent experiments. Data in H represent mean values from three independent experiments.

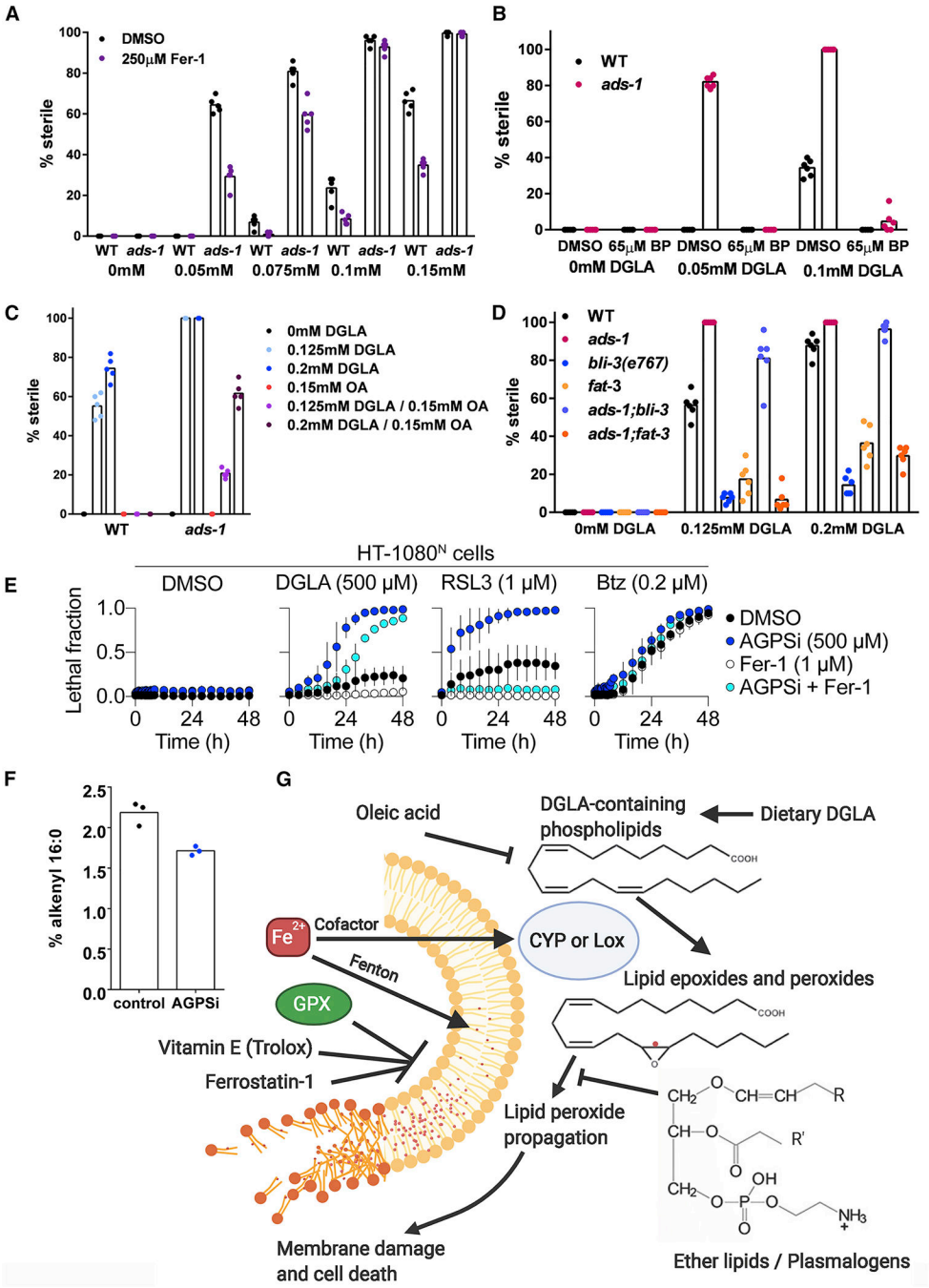

Figure 3. Ether lipids protect cells from ferroptosis.

(A) Percentage (%) sterility of wild-type and *ads-1* on various doses of DGLA and ferrostatin-1 (Fer-1). (B) Iron chelation by 2,2-bipiridine suppresses ferroptosis in both wild type and in *ads-1* mutants. (C) Dietary oleic acid partially suppresses the sterility induced by DGLA in *ads-1* mutants. C) Epistasis analysis of *ads-1* combined with *bli-3* or *fat-3.* In figures 3A-3D, each point represents the % of worms that are sterile in an independent experiment comprising 50 worms for each treatment. Statistical significance was determined by two-way ANOVA with a Tukey's test for multiple comparisons (Table S1). Fatty acid

composition data is reported in Table S2. (E) HT-1080^{N} cells were pretreated with DMSO or ZINC-69435460 (AGPSi, 500 μM) for 24 h, then co-treated as indicated. Data are mean ± SD of three independent experiments. (F) The plasmalogen species, 16:0 alkenyl, is reduced in cells treated with AGPSi (500 μM). (G) Model for dietary DGLA-induced ferroptosis.

Table 1.

Common features of DGLA-induced germ cell death and mammalian ferroptosis

Feature of Ferroptosis	**Mammalian Ferroptosis**	**DGLA-induced germ cell death in *C. elegans***
Involvement of toxic metabolite derived from omega-6 PUFA	Exogenous omega-6 PUFAs sensitizes cells to ferroptosis (Doll et al., 2017). DGLA induces ferroptosis in HT-1080 cells (Figure 2A, B, C, D, G).	Germ cell death induced by dietary omega-6 PUFAs DGLA and AA (Figs. 2, 3, 5 from (Watts and Browse, 2006)).
Involvement of oxidized PUFAs	Oxidized AA-PE and Ada-PE cause cell death (Kagan et al., 2017; Zou et al., 2020).	CYP450 produces toxic epoxides derived from DGLA (Figs. 2, 3, 4 from (Deline et al., 2015)).
Glutathione and oxidative stress resistance pathways (NRF2) protect from ferroptosis	Involvement of glutathione and GPX4 (Ingold et al., 2018; Seiler et al., 2008; Yang et al., 2014). Nrf2 protects cells from ferroptosis (Fan et al., 2017; Sun et al., 2016).	Mutations in glutathione synthesis genes sensitizes worms to DGLA-induced sterility. SKN-1 (NRF2) protects against cell death (Figs. 1, 2, 3, and 4 from (Webster et al., 2013)). The *gpx-1* mutants are sensitive to DGLA-induced sterility (Figure 1F).
Apoptotic pathway not required	Caspase independence of ferroptosis (Dixon et al., 2012; Dolma et al., 2003)	DGLA-induced cell death occurs in apoptosis-defective mutants (Fig. 5 from (Webster et al., 2013), Figure 1A).
Specific inhibition by ferrostatin-1, iron chelators, and antioxidants.	Inhibition by ferrostatin-1 and iron chelators (Dixon et al., 2012; Skouta et al., 2014). Inhibition by antioxidants (Dixon et al., 2012; Matsushita et al., 2015; Yang and Stockwell, 2008, 2016)	DGLA-induced germ cell death is suppressed by ferrostain-1, vitamin E, and iron chelators (Figure 1A, B, C, D, E, H).
Promotion of cell death by NADPH oxidase	NOX inhibitors suppress ferroptosis (Dixon et al., 2012)	*bli-3* mutants are resistant to DGLA-induced sterility (Figure 1G).
MUFAs protect from ferroptosis	MUFAs protect HT-1080 cells from erastin-induced ferroptosis (Magtanong et al., 2019)	Exogenous and endogenous MUFAs protect germ cells from DGLA-induced cell death (Figure 1I and J).
Endogenous ether lipids protect from DGLA-induced ferroptosis	AGPS inhibitor treatment renders HT-1080 cells sensitive to erastin or DGLA-induced ferroptosis (Figure 3E)	Ether lipid-deficient mutants are sensitive to DGLA-induced germ cell death (Figure 3A, B, C, D)